Moving Sampling Schemes for 2D DOA Estimation Using Sparse Planar Arrays

Yibin Liang, Zhi Zheng, Hui Chen, *Member, IEEE*, and Jie Zhuang

***Abstract*—In this letter, we devise two moving sampling schemes for two-dimensional (2D) direction-of-arrival (DOA) estimation using sparse planar arrays. The proposed schemes are applied to two different kinds of sparse planar arrays on a moving platform. By designing the appropriate motion trail, the proposed schemes can joint the uniform rectangular parts of the synthetic difference coarray together to yield a larger uniform rectangular array (URA). Compared with the traditional virtual array construction, our schemes can generate a larger virtual URA, and thus result in a significant increase in the number of uniform degrees of freedom (DOFs). Numerical results demonstrate the advantages of the proposed schemes in the number of uniform DOFs and DOA estimation accuracy.**

***Index Terms*—2D DOA estimation, array motion, sparse planar array, synthetic array, synthetic difference coarray.**

I. Introduction

In ARRAY signal processing, direction-of-arrival (DOA) estimation of targets-of-interest has been an important problem with numerous application areas, including radar, communication, and electronic warfare [1], [2]. For two-dimensional (2D) DOA estimation, the most popular array is uniform rectangular array (URA) where the inter-sensor spacings are not more than half wavelength to obtain unambiguous estimation [3]. However, the array aperture and degrees of freedom (DOFs) of URAs are limited by the sensor number. Furthermore, it is sensitive to mutual coupling effects due to small inter-sensor spacings.

To address these issues, sparse planar arrays have attracted much attention in the field of 2D DOA estimation. By exploiting the difference coarray, sparse planar arrays can achieve an increased number of DOFs. Moreover, their inter-sensor spacings are not limited by half-wavelength, which significantly reduces mutual coupling effects. To increase the number of DOFs, several 2D sparse arrays with hole-free difference coarrays have been suggested, including billboard arrays [4], open-box arrays (OBA) [5] and nested planar arrays (NPA) [6]. Moreover, several derivatives of OBA have been designed to reduce mutual coupling, including the partially OBA (POBA), half OBA (HOBA), HOBA with two layers (HOBA-2), and hourglass array [7], [8].

Received 5 December 2025; revised 19 January 2026; accepted 20 January 2026. Date of publication 23 January 2026; date of current version 4 February 2026. This work was supported by the Natural Science Foundation of Sichuan Province under Grant 2026NSFSC0395. The associate editor coordinating the review of this article and approving it for publication was Prof. Zhiguo Shi. *(Corresponding author: Zhi Zheng.)*

The authors are with the School of Information and Communication Engineering, University of Electronic Science and Technology of China, Chengdu 611731, China (e-mail: 202321010913@std.uestc.edu.cn; zz@uestc.edu.cn; huichen0929@uestc.edu.cn; huichen0929@uestc.edu.cn).

Digital Object Identifier 10.1109/LSP.2026.3657182

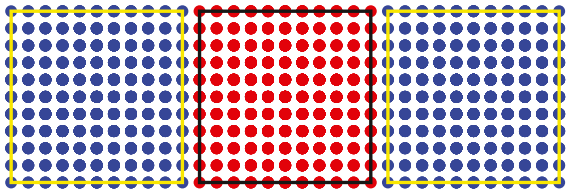

Fig. 1. Synthetic difference coarray of URA with $N_x = N_y = 6$. Red bullets: difference coarray. Blue bullets: cross-difference coarray.

To reduce further mutual coupling, half H arrays and ladder arrays [9] are also proposed. Moreover, coprime planar arrays (CPA) [10] and several improved structures of CPA [11], [12], [13] are developed.

Recently, synthetic aperture processing (SAP) is applied to sparse arrays to increase the array aperture and the number of DOFs. In [14], SAP technology is applied to coprime arrays with coprime integers M and N. By moving $N/2$ half wavelengths, SAP technology enable coprime arrays to yield a hole-free difference coarray. Qin et al. [15] design the dilated nested array and apply SAP technology to the dilated nested array for DOA estimation. In [16], the motion of various typical sparse arrays is utilized for increasing the number of DOFs. However, the improvement of DOFs by half-wavelength motion is quite limited. In [17], a new approach for virtual array construction exploiting sparse array motion is developed, and this approach can increase the number of DOFs by three times. In [18], an improved moving scheme for DOA estimation using coprime arrays is proposed. The improved scheme is superior to [16] and [17]. Wu et al. [19] developed nonuniform moving sampling schemes for DOA estimation on a moving platform. By optimizing the consecutive coarray segment, these schemes achieve higher estimation accuracy and number of DOFs than the previous schemes. In [20], two kinds of array motion strategies are designed to improve the uniform DOFs and DOA estimation accuracy of the CADiS. In [21], [22], [23], the vertical motion of coprime linear array or arbitrary sparse linear array for 2D DOA estimation is discussed. Nevertheless, all the above-mentioned schemes focus on sparse linear arrays, while the motion of sparse planar arrays is never addressed. Unlike sparse linear arrays, sparse planar arrays have difference coarrays with different structures. Accordingly, the impacts of array motion on the uniform DOFs of sparse planar arrays are different with that of sparse linear arrays. Therefore, the moving schemes of sparse planar arrays need to be specially designed for applying SAP technology.

In this letter, we suggest two moving sampling schemes for 2D DOA estimation with sparse planar arrays. By designing the proper motion trail, the proposed schemes can joint the uniform

rectangular parts of the synthetic difference coarray together to form a larger virtual URA. Compared with the traditional difference coarray construction, our schemes can yield a larger virtual URA segment, and thus increase significantly the number of uniform DOFs. Numerical results validate the proposed schemes for improving the number of resolvable sources and DOA estimation accuracy.

II. Preliminaries

A. Array Signal Model

Consider a Q-sensor planar array moving at a constant velocity vector $\mathbf{v} = (v_x, v_y)$. The sensor positions of the array are represented as $\mathbb{P} = [\mathbf{p}_1, \ldots, \mathbf{p}_Q]^T d$, where $\mathbf{p}_q = (x_q, y_q) \in \mathbb{Z}^2$ $(q = 1, 2, \ldots, Q)$ and $d = \lambda/2$ denotes the minimum distance between sensors with λ being the signal wavelength. Assume K far-field, uncorrelated signals impinge on this array from distinct 2D directions $\{(\theta_k, \varphi_k)\}_{k=1}^K$, where $\theta_k \in [0, 2\pi]$ and $\varphi_k \in [0, \pi/2]$ are the azimuth and elevation angles of the kth source, respectively. Due to the assumed short-time of array motion, the 2D directions of sources with respect to this array can be regarded as constant angles. The array output vector at time t is given by:

$$\mathbf{x}(t) = \mathbf{A}\mathbf{s}(t) + \mathbf{n}(t) \tag{1}$$

where $\mathbf{s}(t)$ denotes the signal vector given by

$$\begin{aligned}\mathbf{s}(t) = [&s_1(t)\exp\left(-j2\pi t\left(v_x\cos\alpha_1 + v_y\cos\beta_1\right)/\lambda\right),\\ &s_2(t)\exp\left(-j2\pi t\left(v_x\cos\alpha_2 + v_y\cos\beta_2\right)/\lambda\right),\ldots,\\ &s_K(t)\exp\left(-j2\pi t\left(v_x\cos\alpha_K + v_y\cos\beta_K\right)/\lambda\right)]^T\end{aligned} \tag{2}$$

with $\cos\alpha_k = \cos\theta_k \sin\varphi_k$ and $\cos\beta_k = \sin\theta_k \sin\varphi_k$, $\mathbf{n}(t)$ is the noise vector, and $\mathbf{A} = [\mathbf{a}(\alpha_1, \beta_1), \ldots, \mathbf{a}(\alpha_K, \beta_K)] \in \mathbb{C}^{Q\times K}$ is the array manifold matrix with

$$\begin{aligned}\mathbf{a}(\alpha_k, \beta_k) = [&1, \exp\left(-j2\pi d/\lambda\left(x_2\cos\alpha_k + y_2\cos\beta_k\right)\right),\\ &\ldots, \exp\left(-j2\pi d/\lambda\left(x_Q\cos\alpha_k + y_Q\cos\beta_k\right)\right)]^T.\end{aligned} \tag{3}$$

At time $t + \tau$, the observed signal of the array becomes

$$\mathbf{x}(t+\tau) = \bar{\mathbf{A}}\mathbf{s}(t+\tau) + \mathbf{n}(t+\tau) \tag{4}$$

where $\bar{\mathbf{A}} = [\bar{\mathbf{a}}(\alpha_1, \beta_1), \ldots, \bar{\mathbf{a}}(\alpha_K, \beta_K)] \in \mathbb{C}^{Q\times K}$, with

$$\begin{aligned}\bar{\mathbf{a}}(\alpha_k, \beta_k) = &\exp\left(-j2\pi\tau\left(v_x\cos\alpha_k + v_y\cos\beta_k\right)/\lambda\right)\\ &\cdot \mathbf{a}(\alpha_k, \beta_k)\end{aligned} \tag{5}$$

$$\begin{aligned}\mathbf{s}(t+\tau) = [&s_1(t+\tau)\exp\left(-j2\pi t\left(v_x\cos\alpha_1 + v_y\cos\beta_1\right)/\lambda\right),\\ &s_2(t+\tau)\exp\left(-j2\pi t\left(v_x\cos\alpha_2 + v_y\cos\beta_2\right)/\lambda\right),\ldots,\\ &s_K(t+\tau)\exp\left(-j2\pi t\left(v_x\cos\alpha_K + v_y\cos\beta_K\right)/\lambda\right)]^T\end{aligned} \tag{6}$$

For narrowband signals with central frequency f, $s_k(t+\tau) = s_k(t)\exp(j2\pi f\tau)$. Hence, $\mathbf{x}(t+\tau)$ can be rewritten as:

$$\mathbf{x}(t+\tau) = \exp(j2\pi f\tau)\bar{\mathbf{A}}\mathbf{s}(t) + \mathbf{n}(t+\tau) \tag{7}$$

By multiplying by a phase correction factor $\exp(-j2\pi f\tau)$, we get the phase synchronized observed signal vector [24]:

$$\tilde{\mathbf{x}}(t+\tau) = \exp(-j2\pi f\tau)\mathbf{x}(t+\tau) = \bar{\mathbf{A}}\mathbf{s}(t) + \tilde{\mathbf{n}}(t+\tau) \tag{8}$$

where $\tilde{\mathbf{n}}(t+\tau) = \exp(-j2\pi f\tau)\mathbf{n}(t+\tau)$.

Combining (1) and (8) yields the synthetic array signal:

$$\mathbf{y}(t) = \begin{bmatrix}\mathbf{x}(t)\\ \tilde{\mathbf{x}}(t+\tau)\end{bmatrix} = \mathbf{B}\mathbf{s}(t) + \boldsymbol{\varepsilon}(t) \tag{9}$$

where $\mathbf{B} = [\mathbf{A}^T, \bar{\mathbf{A}}^T]^T$, and $\boldsymbol{\varepsilon}(t) = [\mathbf{n}^T(t), \tilde{\mathbf{n}}^T(t+\tau)]^T$.

B. Synthetic Array and Its Difference Coarray

Assume a planar array specified by the set $\mathbb{P}$ moves along trail $\mathbf{m} = (m_x, m_y) = (v_x\tau, v_y\tau)$, the sensor positions of the shifted array are expressed as

$$\bar{\mathbb{P}} = \mathbb{P} + \mathbf{m} = \{\mathbf{p} + \mathbf{m} \mid \mathbf{p} \in \mathbb{P}\}. \tag{10}$$

The sensor positions of the synthetic array of the original and the shifted arrays are given by

$$\mathbb{P}_{\text{sa}} = \mathbb{P} \cup \bar{\mathbb{P}}. \tag{11}$$

Since $\mathbb{P}$ and $\bar{\mathbb{P}}$ have the same difference coarray, the synthetic difference coarray of $\mathbb{P}$ is expressed as

$$\mathbb{D}_{\text{sa}} = \mathbb{D} \cup \mathbb{D}_c \tag{12}$$

where $\mathbb{D} = \{\mathbf{p}_1 - \mathbf{p}_2 = \mathbf{l} \mid \mathbf{p}_1, \mathbf{p}_2 \in \mathbb{P}\}$ is the difference coarray of $\mathbb{P}$ with $\mathbf{l} = (l_x, l_y) \in \mathbb{Z}^2$, and $\mathbb{D}_c$ denotes the cross-difference coarray between $\mathbb{P}$ and $\bar{\mathbb{P}}$ defined as

$$\mathbb{D}_c = \left\{(\mathbf{p}_1 - \mathbf{p}_2) \cup (\mathbf{p}_2 - \mathbf{p}_1) \mid \mathbf{p}_1 \in \mathbb{P}, \mathbf{p}_2 \in \bar{\mathbb{P}}\right\}. \tag{13}$$

According to (10) and (13), $\mathbb{D}_c$ can be expressed as

$$\mathbb{D}_c = \left\{(\mathbf{l} + \mathbf{m}) \cup (\mathbf{l} - \mathbf{m}) \mid \mathbf{l} \in \mathbb{D}\right\}. \tag{14}$$

III. Proposed Moving Sampling Schemes

A. The First Moving Sampling Scheme

The first moving scheme is aimed at a planar array whose difference coarray only includes one virtual URA, such as URA, BA and OBA. Denoting the virtual URA as:

$$\mathbb{U} = \left\{(l_x, l_y) \in \mathbb{Z}^2 \mid l_x \in [-N, N],\ l_y \in [-M, M]\right\}, \tag{15}$$

the array is assumed to move along trail $\mathbf{m} = ((2N+1)d, 0)$.

About the first scheme, we have the following theorem.

Theorem 1: For a planar array $\mathbb{P}$ moving along trail $\mathbf{m} = (m_x, m_y) = ((2N+1)d, 0)$, the difference coarray of $\mathbb{P}_{\text{sa}} = \mathbb{P} \cup \bar{\mathbb{P}}$ has an uniform rectangular segment:

$$\begin{aligned}\mathbb{U}_{\text{sa}} = \{(l_x, l_y) \in \mathbb{Z}^2 \mid &l_x \in [-(3N+1), 3N+1],\\ &l_y \in [-M, M]\}.\end{aligned} \tag{16}$$

where $\mathbb{U}_{\text{sa}}$ is the largest central URA of $\mathbb{D}_{\text{sa}}$.

Proof 1: Since the planar array moves along the x-axis, we only need to consider the consecutive lag ranges of $\mathbb{D}_{\text{sa}}$ in the x-axis direction. According to (14) and (15), the cross-difference coarray $\mathbb{D}_c$ has two consecutive segments:

$$\begin{aligned}\mathbb{U}_{c1} = \{(l_x, l_y) \in \mathbb{Z}^2 \mid &\\ &l_x \in [-3N-1, -N-1],\ l_y \in [-M, M]\}\end{aligned} \tag{17}$$

$$\begin{aligned}\mathbb{U}_{c2} = \{(l_x, l_y) \in \mathbb{Z}^2 \mid &\\ &l_x \in [N+1, 3N+1],\ l_y \in [-M, M]\}\end{aligned} \tag{18}$$

Let $\mathbb{U}_c = \mathbb{U}_{c1} \cup \mathbb{U}_{c2}$, the contiguous part of $\mathbb{D}_{\text{sa}}$ is:

$$\mathbb{U}_{\text{sa}} = \mathbb{U} \cup \mathbb{U}_c = \{(l_x, l_y) \in \mathbb{Z}^2 \mid l_x \in [-(3N+1), 3N+1], \; l_y \in [-M, M]\}. \tag{19}$$

Therefore, Theorem 1 has been proven.

Remark 1: The number of uniform DOFs [6] for $\mathbb{P}_{\text{sa}}$ is $3(2M+1)(2N+1)$. Clearly, the number of uniform DOFs has increased threefold by applying the first moving scheme.

Remark 2: When the planar array moves along trail $\mathbf{m} = (m_x, m_y) = (0, (2M+1)d)$, the number of uniform DOFs can also be increased by three times.

Fig. 1 displays the synthetic difference coarray of the 36-element URA by exploiting array motion. It is seen that the cross-difference coarray is connected with the difference coarray to form the synthetic difference coarray, i.e., a larger virtual URA. More specifically, the size of the virtual URA is exactly three times that of the original difference coarray.

B. The Second Moving Sampling Scheme

For some 2D sparse arrays, such as nested and coprime arrays, there exist two overlapping symmetric URAs in the resulting difference coarray $\mathbb{D}$. To fully utilize these virtual URAs, we propose another moving sampling scheme.

From the two overlapping virtual URAs, we extract two adjacent URAs defined as:

$$\mathbb{U}_1 = \{(l_x, l_y) \in \mathbb{Z}^2 \mid l_x \in [-N, L], \; l_y \in [0, M]\} \tag{20}$$

$$\mathbb{U}_2 = \{(l_x, l_y) \in \mathbb{Z}^2 \mid l_x \in [-L, N], \; l_y \in [-M, 0]\} \tag{21}$$

where L, M and N are positive integers.

In this scheme, we assume that the array moves along trail $\mathbf{m} = ((L+N+1)d, 0)$. With regard to the second scheme, we give the following theorem.

Theorem 2: For a 2D sparse array $\mathbb{P}$ moving along trail $\mathbf{m} = (m_x, m_y) = ((L+N+1)d, 0)$, the difference coarray of $\mathbb{P}_{\text{sa}} = \mathbb{P} \cup \bar{\mathbb{P}}$ has the largest central URA given as

$$\mathbb{U}_{\text{sa}} = \{(l_x, l_y) \in \mathbb{Z}^2 \mid l_x \in [-2b-a-1, 2b+a+1], \; l_y \in [-M, M]\} \tag{22}$$

where $a = \max(L, N)$ and $b = \min(L, N)$.

Proof 2: According to (14) and (20), the synthetic array of $\mathbb{U}_1$ after moving $(L+N+1)d$ along the x-axis is given as

$$\mathbb{U}_{\text{sa1}} = \{(l_x, l_y) \in \mathbb{Z}^2 \mid l_x \in [-2N-L-1, 2L+N+1], \; l_y \in [0, M]\} \tag{23}$$

According to (14) and (21), the synthetic array of $\mathbb{U}_2$ after moving $(L+N+1)d$ along the x-axis is given as

$$\mathbb{U}_{\text{sa2}} = \{(l_x, l_y) \in \mathbb{Z}^2 \mid l_x \in [-2L-N-1, 2N+L+1], \; l_y \in [-M, 0]\} \tag{24}$$

When $L \geq N > 0$, we can derive from $\mathbb{U}_{\text{sa1}} \cup \mathbb{U}_{\text{sa2}}$ a virtual URA defined as:

$$\mathbb{U}_{\text{sa}} = \{(l_x, l_y) \in \mathbb{Z}^2 \mid l_x \in [-2N-L-1, 2N+L+1], \; l_y \in [-M, M]\} \tag{25}$$

When $N > L > 0$, we can derive from $\mathbb{U}_{\text{sa1}} \cup \mathbb{U}_{\text{sa2}}$ another virtual URA defined as:

$$\mathbb{U}_{\text{sa}} = \{(l_x, l_y) \in \mathbb{Z}^2 \mid l_x \in [-2L-N-1, 2L+N+1], \; l_y \in [-M, M]\} \tag{26}$$

Combining (25) with (26), we can derive (22).

Remark 3: The uniform DOFs of the synthetic array is $(4b+2a+3)(2M+1)$, while the uniform DOFs of the original array is $(2b+1)(2M+1)$. Thus, the number of uniform DOFs is significantly increased by applying the above moving scheme.

Remark 4: When the 2D sparse array moves along trail $\mathbf{m} = (m_x, m_y) = (0, v_y\tau)$, and $v_y\tau$ is equal to the length of the largest URA of $\mathbb{D}$ in the y-axis direction, the number of uniform DOFs can still be increased by the same magnitude.

The synthetic difference coarray of the 17-element NPA is shown in Fig. 2. We observe that the uniform rectangular parts of the cross-difference coarray are connected to that of the original difference coarray, so that the synthetic difference coarray includes a larger central URA. More specifically, the size of the largest URA in the synthetic difference coarray is more than three times that of the original difference coarray.

Table I shows the number of uniform DOFs for six kinds of 2D arrays after applying moving schemes. We see that the synthetic URA, BA, OBA and HOBA-2 offer three times the uniform DOFs of the original arrays. It is also seen that the synthetic NPA and CPA increase the uniform DOFs by more than three times compared to their original counterparts.

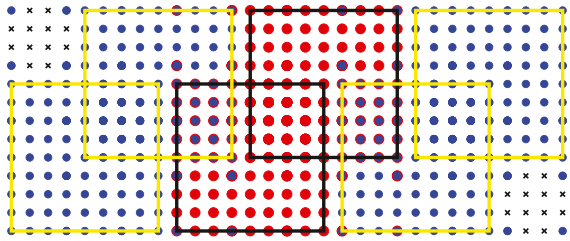

Fig. 2. Synthetic difference coarray of NPA with $N_1 = N_2 = 3$. Red bullets: difference coarray. Blue bullets: cross-difference coarray. Crosses: holes.

TABLE I
A SUMMARY OF UNIFORM DOFS FOR SIX KINDS OF 2D ARRAYS

Array configuration	Array parameter	Uniform DOFs	
		original	synthetic
URA	$N_x = N_y = 5$	81	243
BA	$N_x = N_y = 13$	625	1875
OBA	N_x=18, N_y=10	665	1995
HOBA-2	N_x=18, N_y=10	665	1995
NPA	$N_1 = 4$, $N_2 = 5$	231	1551
CPA	$M = 4$, $N = 5$	119	527

IV. NUMERICAL RESULTS

We conduct numerical simulations to illustrate the original and synthetic URA, BA, NPA and CPA in terms of detection capability and DOA estimation accuracy. For the investigated arrays, we set the parameters as shown in Table I. For all the arrays, the unitary ESPRIT approach [25] is applied to their original difference and synthetic difference coarrays to find the 2D DOAs. In all simulations, we consider K equal-power sources, whose normalized 2D DOAs are generated according to [8]. For each figure, 200 Monte-Carlo trials are performed.

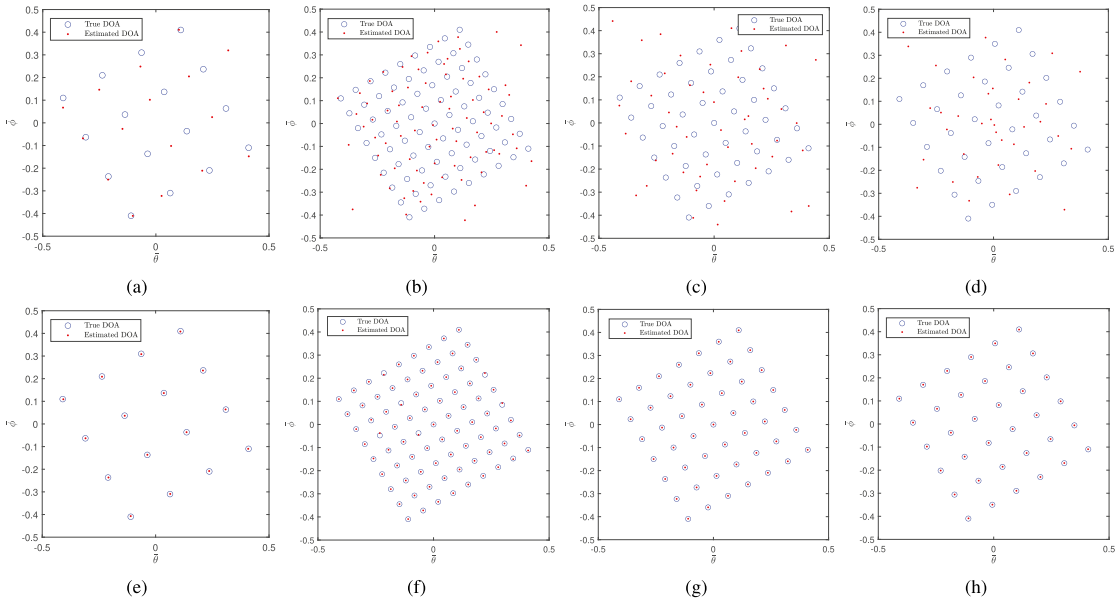

Fig. 3. Distribution of 2D DOA estimation. SNR $= -20$ dB and $T = 1000$. (a) Original URA, $K = 16$. (b) Original BA, $K = 81$. (c) Original NPA, $K = 49$. (d) Original CPA, $K = 36$. (e) Synthetic URA, $K = 16$. (f) Synthetic BA, $K = 81$. (g) Synthetic NPA, $K = 49$. (h) Synthetic CPA, $K = 36$.

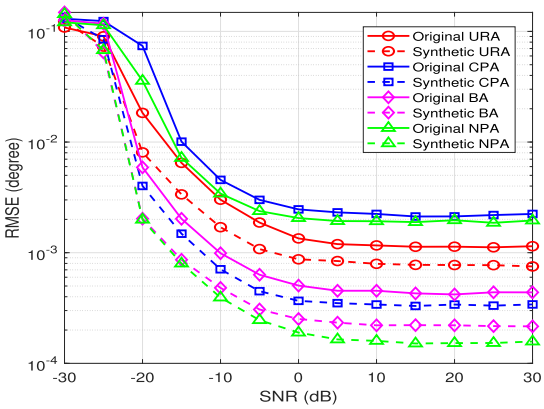

Fig. 4. RMSE of estimated normalized 2D DOAs versus SNR for $K = 9$ uncorrelated sources. $T = 1000$.

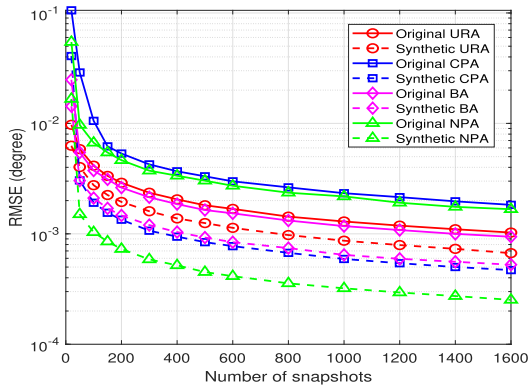

Fig. 5. RMSE of estimated normalized 2D DOAs versus snapshot number for $K = 9$ uncorrelated sources. SNR $= 0$ dB.

First, we examine the detection capability of the original and synthetic arrays for multiple sources. When $K = 16, 36, 49, 81$ sources, the distribution of average 2D DOA estimates is demonstrated in Fig. 3, where the SNR is fixed at -20 dB and the number of snapshots is set as $T = 1000$. It is observed from Figs. 3(a)–3(d) that the original URA, BA, NPA, and CPA fail to detect all the sources. In comparison, the synthetic URA, BA, NPA, and CPA can resolve all the sources, as depicted in Figs. 3(e)–3(h). That is because the synthetic arrays employing moving sampling schemes provide a high number of uniform DOFs than their original counterparts. Second, we compare the RMSE performance of the original and synthetic arrays. When $K = 9$ sources, the RMSE of the estimated normalized 2D DOAs against SNR at $T = 1000$ is shown in Fig. 4, from which we notice that the synthetic URA, BA, NPA, and CPA achieve smaller RMSEs than the original counterparts. Moreover, among all the arrays, the RMSE reduction of the NPA and CPA is more obvious after moving sampling scheme is applied. When $K = 9$ sources, the RMSE of the estimated normalized 2D DOAs versus snapshot number at SNR $= 0$ dB is plotted in Fig. 5. It is seen that the numerical results are consistent with those of Fig. 4. The synthetic URA, BA, NPA, and CPA provide higher estimation accuracy than the original counterparts.

V. Conclusion

In this letter, we have presented two moving sampling schemes for 2D DOA estimation using sparse planar arrays. These proposed schemes are applicable to two different kinds of sparse planar arrays. Based on the specific difference coarray structure, the proposed schemes utilize the appropriate moving trail to maximize the uniform rectangular part of the synthetic difference coarray. It has been proved that the proposed schemes can enhance greatly the achievable DOFs of sparse planar arrays. Numerical results indicate that our schemes can significantly improve the number of resolvable sources and DOA estimation accuracy.

REFERENCES

[1] Z. Zheng, Y. Huang, W.-Q. Wang, and H. C. So, "Augmented covariance matrix reconstruction for DOA estimation using difference coarray," *IEEE Trans. Signal Process.*, vol. 69, pp. 5345–5358, 2021.

[2] H. Zheng, C. Zhou, Z. Shi, Y. Gu, and Y. D. Zhang, "Coarray tensor direction-of-arrival estimation," *IEEE Trans. Signal Process.*, vol. 71, pp. 1128–1142, 2023.

[3] C. Zhou, Y. Gu, Z. Shi, and M. Haardt, "Structured Nyquist correlation reconstruction for DOA estimation with sparse arrays," *IEEE Trans. Signal Process.*, vol. 71, pp. 1849–1862, 2023.

[4] R. T. Hoctor and S. A. Kassam, "The unifying role of the coarray in aperture synthesis for coherent and incoherent imaging," *Proc. IEEE*, vol. 78, no. 4, pp. 735–752, Apr. 1990.

[5] C. R. Greene and R. C. Wood, "Sparse array performance," *J. Acoustical Soc. Amer.*, vol. 63, no. 6, pp. 1866–1872, 1978.

[6] P. Pal and P. P. Vaidyanathan, "Nested arrays in two dimensions, part I: Geometrical considerations," *IEEE Trans. Signal Process.*, vol. 60, no. 9, pp. 4694–4705, Sep. 2012.

[7] C.-L. Liu and P. P. Vaidyanathan, "Two-dimensional sparse arrays with hole-free coarray and reduced mutual coupling," in *Proc. Asilomar Conf. Signals, Syst., Comput.*, Pacific Grove, CA, USA, Nov. 2016, pp. 1508–1512.

[8] C.-L. Liu and P. P. Vaidyanathan, "Hourglass arrays and other novel 2-D sparse arrays with reduced mutual coupling," *IEEE Trans. Signal Process.*, vol. 65, no. 13, pp. 3369–3383, Jul. 2017.

[9] S. Ren, X. Li, X. Luo, and W. Wang, "Extensions of open box array with reduced mutual coupling," *IEEE Sensors J.*, vol. 18, no. 13, pp. 5475–5484, Jul. 2018.

[10] Q. Wu, F. Sun, P. Lan, G. Ding, and X. Zhang, "Two-dimensional direction-of-arrival estimation for co-prime planar arrays: A partial spectral search approach," *IEEE Sensors J.*, vol. 16, no. 14, pp. 5660–5670, Jul. 2016.

[11] W. Zheng, X. Zhang, and H. Zhai, "Generalized coprime planar array geometry for 2-D DOA estimation," *IEEE Commun. Lett.*, vol. 21, no. 5, pp. 1075–1078, May 2017.

[12] X. Yang, Y. Wang, and P. Chargé, "Hole locations and a filling method for coprime planar arrays for DOA estimation," *IEEE Commun. Lett.*, vol. 25, no. 1, pp. 157–160, Jan. 2021.

[13] W. Tong, Z. Zheng, W.-Q. Wang, and H. C. So, "Symmetric displaced coprime planar array for two-dimensional direction-of-arrival estimation," *IEEE Sensors J.*, vol. 22, no. 23, pp. 23221–23231, Dec. 2022.

[14] J. Ramirez Jr and J. L. Krolik, "Synthetic aperture processing for passive co-prime linear sensor arrays," *Digit. Signal Process.*, vol. 61, pp. 62–75, Feb. 2017.

[15] G. Qin, Y. D. Zhang, and M. G. Amin, "DOA estimation exploiting moving dilated nested arrays," *IEEE Signal Process. Lett.*, vol. 26, no. 3, pp. 490–494, Jan. 2019.

[16] G. Qin, M. G. Amin, and Y. D. Zhang, "DOA estimation exploiting sparse array motions," *IEEE Trans. Signal Process.*, vol. 67, no. 11, pp. 3013–3027, Jun. 2019.

[17] S. Li and X.-P. Zhang, "A new approach to construct virtual array with increased degrees of freedom for moving sparse arrays," *IEEE Signal Process. Lett.*, vol. 27, pp. 805–809, 2020.

[18] Y. Zhang, J. Shi, H. Zhou, G. Hu, and T. Ma, "Improved moving scheme for coprime arrays in direction of arrival estimation," *Digit. Signal Process.*, vol. 149, Jun. 2024, Art. no. 104514.

[19] H. Wu, Q. Shen, W. Cui, and W. Liu, "DOA estimation with nonuniform moving sampling scheme based on a moving platform," *IEEE Signal Process. Lett.*, vol. 28, pp. 1714–1718, 2021.

[20] P. Ma, J. Li, J. Pan, X. Zhang, and R. Gil-Pita, "Enhanced DOA estimation with augmented CADiS by exploiting array motion strategies," *IEEE Trans. Veh. Technol.*, vol. 72, no. 4, pp. 4713–4727, Apr. 2023.

[21] J. Chu, Z. Zhang, Y. Huang, and Y. Guo, "A novel approach of 2-D DOA estimation by employing coprime linear array motion," *IEEE Commun. Lett.*, vol. 26, no. 1, pp. 69–73, Jan. 2022.

[22] G. Wang, Z. Fei, and S. Ren, "2D DOA estimation exploiting vertical synthetic planar arrays," *IEEE Access*, vol. 9, pp. 3497–3507, 2020.

[23] J. Chu, Z. Zhang, and Y. Guo, "Exploration on 2D DOA estimation of linear array motion: Uniform linear motion," *China Commun.*, vol. 20, no. 11, pp. 78–95, Nov. 2023.

[24] S. Stergiopoulos and E. J. Sullivan, "Extended towed array processing by an overlap correlator," *J. Acoustical Soc. Amer.*, vol. 86, no. 1, pp. 158–171, 1989.

[25] M. D. Zoltowski, M. Haardt, and C. P. Mathews, "Closed-form 2-D angle estimation with rectangular arrays in element space or beamspace via unitary ESPRIT," *IEEE Trans. Signal Process.*, vol. 44, no. 2, pp. 316–328, Feb. 1996.